Hindawi Publishing Corporation
Mathematical Problems in Engineering
Volume 2013, Article ID 473495, 10 pages
http://dx.doi.org/10.1155/2013/473495

Research Article

Modeling and Analysis of the Weld Bead Geometry in Submerged Arc Welding by Using Adaptive Neurofuzzy Inference System

Nuri Akkas,[1] Durmuş Karayel,[2] Sinan Serdar Ozkan,[2] Ahmet Oğur,[3] and Bayram Topal[4]

[1] *Faculty of Technical Education, Sakarya University, Sakarya, Turkey*
[2] *Department of Mechatronics Engineering, Faculty of Technology, Sakarya University, Sakarya, Turkey*
[3] *Department of Mechanical Engineering, Faculty of Engineering, Sakarya University, Sakarya, Turkey*
[4] *Department of Business, Faculty of Business, Sakarya University, Sakarya, Turkey*

Correspondence should be addressed to Durmuş Karayel; dkarayel@sakarya.edu.tr

Received 30 May 2013; Revised 29 August 2013; Accepted 13 September 2013

Academic Editor: Saeed Balochian

This study is aimed at obtaining a relationship between the values defining bead geometry and the welding parameters and also to select optimum welding parameters. For this reason, an experimental study has been realized. The welding parameters such as the arc current, arc voltage, and welding speed which have the most effect on bead geometry are considered, and the other parameters are held as constant. Four, three, and five different values for the arc current, the arc voltage, and welding speed are used, respectively. So, sixty samples made of St 52-3 material were prepared. The bead geometries of the samples are analyzed, and the thickness and penetration values of the weld bead are measured. Then, the relationship between the welding parameters is modeled by using artificial neural network (ANN) and neurofuzzy system approach. Each model is checked for its adequacy by using test data which are selected from experimental results. Then, the models developed are compared with regard to accuracy. Also, the appropriate welding parameters values can be easily selected when the models improve.

1. Introduction

The submerged arc welding (SAW) is one of the manufacturing methods which are widely used. The mechanical properties of the welding joints are directly dependent on the geometrical form of bead and its properties. At the same time, the form of bead and its properties change according to the process parameters. Therefore, the process parameters must be selected so that an appropriate weld bead can be formed. There is no linear relationship between the welding parameters and weld bead geometry, and empirical formulas and experimental results are generally used for this relation. Most times, this case is incapable to select the optimum parameters values. Therefore, researchers have begun to use artificial intelligence technologies and statistics analysis methods in order for, the optimum parameters values to be selected and the relationship between the values defining bead geometry and welding parameters can be found.

Chandel et al. have developed software for theoretical predictions of the effect of current, electrode polarity, electrode diameter, and electrode extension on the melting rate, bead height, bead width, and weld penetration, in submerged-arc welding. They have predicted the weld bead geometry and melting rates of both the submerged and the metal arc welding processes by this software. The software is based on the algorithms developed by Yang et al. for predicting the weld bead geometry. This model predicts bead geometry for bead-on-plate (BOP) welds only. The variables required for input are current, voltage, travel speed, electrode diameter, electrode extension, and the electrode polarity [1].

Li et al. modeled the nonlinear relationship between the five geometric descriptors (height, width, penetration, fused and deposited areas) of a bead and the welding parameters (current, voltage, and welding speed) of submerged arc welding using neutral networks. They have shown the advantages of single-output networks by a comparative study

between multioutput networks and single-output networks, each modeling one geometric descriptor. The structure of a conventional feed-forward multilayer perception network with a single output is modified to accommodate an offset layer which offsets the inputs. This network, known as the self-adaptive offset network (SAON), has definite advantages over conventional multilayer perception networks. Altogether, 21 single-output neutral networks have been trained for the four types of SAW welds investigated [2].

Gunaraj and Murugan developed an application of response surface methodology for predicting weld bead quality in submerged arc welding of pipes. In their study, the variables for input are open-circuit voltage, wire feed rate, speed, and nozzle-to-plate distance. The variables for output are penetration, reinforcement, bead width, and dilution [3]. Gunaraj and Murugan also investigated the effect of process variables on the area of the heat-affected zone for the bead-on-plate and bead-on-joint in submerged arc welding of pipes by using response surface methodology. The effect of controllable process variables on the heat input and the area of the heat-affected zone (HAZ) for bead-on-plate and bead-on-joint welding was calculated and analyzed using mathematical models developed for the submerged arc welding of pipes [4]. Tušek developed four mathematical models for calculation of melting rate in arc fusion welding with a wire in coil form. The mathematical models permit calculation of melting rate in direct current welding with single-wire and double-wire electrodes (both polarities). For single-wire welding, the models treated have been improved with regard to the ones published in the literature; for twin-wire welding, these are the first models for calculation of melting rate. The mathematical models have already been tested in practice and the results obtained show that they are very accurate, simple, and applicable to practice [5]. Wikle III et al. used sensing technique for penetration depth control of the submerged arc welding process. They investigated the development of a rugged, low cost, and point infrared sensor to monitor. At the end of the study, they maintained constant depth of penetration using the infrared sensor in the presence of these perturbations by feedback control of the welding process parameters [6]. Murugan and Gunaraj studied prediction and control of weld bead geometry and shape relationships in submerged arc welding of pipes. They have developed mathematical models for submerged arc welding of pipes using five-level factorial techniques to predict three critical dimensions of the weld bead geometry and shape relationships. The models were checked for their adequacy and significance by using the F-test and the t-test, respectively. They have presented main and interaction effects of the process variables on bead geometry and shape factors in graphical form [7]. Tarng et al. used the grey-based Taguchi methods to determine submerged arc welding process parameters in hardfacing. They presented a new approach. In this new approach, the grey relational analysis is adopted to solve the submerged arc welding process with multiple weld qualities. They obtained a grey relational grade from the grey relational analysis which is used as the performance characteristic in the Taguchi method [8]. Kanjilal et al. investigated combined effect of flux and welding parameters on chemical composition and mechanical properties of submerged arc weld metal. In this study, rotatable designs based on statistical experiments for mixtures were developed to predict the combined effect of flux mixture and welding parameters on submerged arc weld metal chemical composition and mechanical properties by second-order regression model. Bead-on-plate weld deposits on low carbon steel plates were made at different flux composition and welding parameter combinations. The variables for input are current, voltage, welding speed, electrode stick-out, and polarity. The variables for output are chemical composition, yield strength, ultimate tensile strength, percent elongation, and Charpy impact toughness and hardness [9].

Nart and Celik propose a new practical approach in modeling to catch the correct shape of the weld pool. They predict temperature distributions and residual stresses for a plate using user subroutines and observe that the finite element results get closer to those of experimental measurements as mesh size gets finer. The residual stresses have been estimated well enough for irregular bead cross-sections by using the new approach for finite element modeling of arc-welding process [10]. Zhao et al. investigated V-I (voltage-current) curve as the monitoring signature to explore a real-time and *in situ* small scale resistance spot welding (SSRSW) quality monitoring method. They performed a systematic research on the V-I curve. Then, they proposed five factors extracted from the V-I curve to estimate the weld quality through an artificial intelligence algorithm. As a result, the study shows that the V-I signature could be used as a reliable [11]. Cho et al. studied the analysis of submerged arc welding process by three-dimensional computational fluid dynamics simulations. In the study, they adopt the Abel inversion method with CCD camera images for direct and alternating current polarities. Then, they validated simulated weld pool profiles with corresponding experimental results and were found to be in good agreement [12].

Acherjee et al. developed a nonlinear model to establish a correlation between the laser transmission welding parameters and output variables by applying artificial neural network (ANN). The process parameters consisted of laser power, welding speed, stand-off distance and clamping pressure, and the output parameters were lap-shear strength and weld-seam width. They used experimental data to train and test the network and then confirm the simulation data obtained from the neural network with the experimental data and, so, show that there was a good agreement between the experimental and numerical results [13]. Shen et al. aimed to determine how variation in heat input achieved was using single and double wires. For this reason, they measured specimens of submerged arc welded plates of ASTM A709 Grade 50 steel considering bead width, penetration depth, contact angle, heat affected zone (HAZ) size, deposition area, penetration area, and total molten area. Then, the level of dilution and different melting efficiencies were analyzed according to measuring results. They showed that the electrode melting efficiency increased initially and then decreased with increasing heat input, but the plate melting efficiency and percentage dilution changed only slightly with it [14]. Leitner et al. studied on the evaluation of fillet weld properties and fatigue

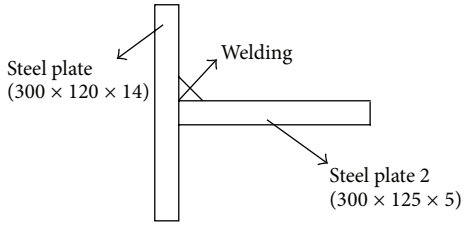

Figure 1: The form of welding joint.

behavior in dependence of welding parameters. They selected weld joints and investigated the influence due to the welding process parameters, especially for high-strength steels, the effect of both the geometrical, and metallurgical notch. Also, they performed the experimental fatigue tests to determine the link between fatigue life and manufacturing process-dependent weld toe notch design. Finally, they adjusted the material and manufacturing properties using the temperature profiles [15]. In this paper, Nagesh and Datta proposed an integrated method with a new approach using experimental design matrix of experimental designs technique. They explained the application of neural network for predicting the weld bead geometric descriptors and the use of genetic algorithm for optimization of process parameters. Also, they attempted to model the welding process for predicting the bead shape parameters of welded joints and used multiple linear regression techniques to develop mathematical models for weld bead shape parameters. In addition, they studied to predict the bead shape parameters using back-propagation neural network and then to optimize the process parameters for the desired front height to front width ratio and back height to back width ratio by applying genetic algorithmic approach [16].

Sathiya et al. investigated the weld bead geometry such as depth of penetration (DP), bead width (BW), and tensile strength (TS) of the laser welded butt joints made of AISI 904L super austenitic stainless steel. They used full factorial design method for the experimental design. Also, they developed artificial neural networks (ANN) program in MATLAB software to establish the relationships between the laser welding input parameters and used genetic algorithm (GA) for optimizing the process parameters and obtained optimum solutions for the three different gases. Also, they validated the optimized parameters with the experimental results [17]. Dhasa and Kumanan study the optimization of parameters of submerged arc weld using nonconventional techniques. In this study, bead-on-plate welds were carried out on mild steel plates using semiautomatic SAW machine. The input-output relationships of the process were carried out by regression analysis, and the weld bead width was minimized by this relationship. Finally, they compared the optimized values obtained from these techniques and obtained a very close relationship between them [18]. Besides these studies, another noteworthy point, in recent times, the researchers have focused their studies on artificial intelligence technologies to analyze the weld seam [19–21].

As seen from the reviewed literature, most of investigations are about bead-on-plate and bead on-joint welds.

Table 1: Welding parameters.

Parameters	Level 1	Level 2	Level 3	Level 4	Level 5
Voltage (Volt)	24	30	36	—	—
Current (Ampere)	200	300	400	500	—
Speed (m/min)	30	40	50	60	70

These methods give a general opinion about the effects of the welding parameters on the bead geometry. however, these effects will change if the joint type changes. Therefore, this study takes into consideration the corner weld of parts with different thickness.

2. Experimental Study

The experiments were conducted at Adapazarı Plants of TIRSAN GROUP. The form and dimension of samples used for the experiment have been presented in Figure 1. The material is a group of structural and constructional steel (St 52-3). There are a lot of parameters which affect weld bead geometry, but this study takes into consideration some of the parameters as welding current, welding voltage, and welding speed because these three parameters are the most effective on the bead geometry.

It is considered that the values of these parameters have been selected from the applicable working ranges. The selected parameters for the welding process are given in Table 1.

The welding rod used is GEKA S2, 3.2 mm diameter, and the welding flux is LINCOLN 761. Fifty-five sets of test plates have been analyzed. The work piece used and the equipment used for the experiment are shown in Figures 2 and 3, respectively.

The length of the work piece welded is 300 mm. However, the length of sample cut from this work piece is 15 mm only, and it is taken from the best quality part of welded work piece. Then, these samples are prepared by the usual metallurgical polishing methods, and their macrostructures are photographed. These photographs are transferred to computer environment. There are thirty-one macrophotographs but some of them are shown in Figure 4, for example.

Also, cross-section of an ideal weld defining the bead geometry is presented in Figure 5. The total penetration area and welding thickness are considered as criterion for bead geometry. A measured graph surface on the computer display is prepared and it is used for measuring welding thickness and defining bead profile.

The welding thickness is directly measured from the macrophotographs. But an indirect method is followed to calculate the penetration area of weld bead. The penetration area of each part is individually considered, and they are expressed as A_1 and A_z. This symbolization is shown in Figure 6.

The coordinates of some points on the limit profiles of weld beads are determined, and these profiles are expressed with polynomial equations. Then, these equations are integrated and so the penetration areas are calculated. Two areas are added and total penetration area is obtained. The

Table 2: Experimental results.

Test number	Welding parameters			Results			
	Current (Ampere)	Voltage (Volts)	Speed (m/min)	Welding thickness (mm)	Penetration area 1 (mm^2) (A1)	Penetration area 2 (mm^2) (A2)	Total area (mm^2) (A1 + A2)
1	200	24	30	5,020	4,344	8,966	13,310
4	200	24	60	3,670	0,514	7,295	7,808
6	200	30	30	5,310	3,205	23,014	26,219
7	200	30	40	4,270	5,261	22,911	28,172
9	200	30	60	3,740	1,727	15,874	17,601
10	200	30	70	2,990	1,551	14,425	15,977
11	200	36	30	5,440	10,607	17,471	28,079
16	300	24	30	7,470	5,877	48,120	53,996
17	300	24	40	6,790	10,450	34,606	45,055
18	300	24	50	5,900	9,487	34,615	44,102
19	300	24	60	4,040	1,282	22,742	24,024
20	300	24	70	2,910	0,920	19,943	20,863
21	300	30	30	6,570	13,365	51,048	64,412
22	300	30	40	5,28	5,014	72,173	77,187
23	300	30	50	4,880	5,431	61,203	66,633
25	300	30	70	4,200	9,497	39,230	48,727
27	300	36	40	6,150	10,853	60,583	71,436
29	300	36	60	5,060	11,509	42,691	54,199
32	400	24	40	7,980	4,735	51,131	55,866
33	400	24	50	7,370	15,228	37,557	52,785
35	400	24	70	6,550	8,285	39,848	48,133
36	400	30	30	8,380	15,061	113,806	128,867
37	400	30	40	7,100	7,859	103,215	111,074
40	400	30	70	4,790	7,432	55,217	62,649
42	400	36	40	7,390	11,439	92,705	104,144
44	400	36	60	5,780	12,174	58,368	70,542
45	400	36	70	5,110	9,906	46,871	56,777
52	500	30	40	11,980	10,291	106,652	116,943
53	500	30	50	11,420	9,440	80,999	90,439
54	500	30	60	8,540	1,112	81,206	82,318
55	500	30	70	7,220	7,815	63,483	71,298

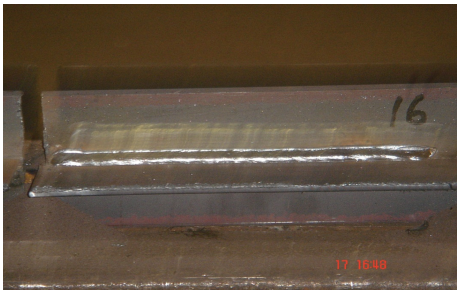

Figure 2: A work piece used for the experiment.

Figure 3: Welding machine used for the experiment.

bead geometry and the polynomial equation of the limit penetration profile of the first sample are shown in Figure 7 and in Figure 8, respectively. The experimental results are presented in Table 2.

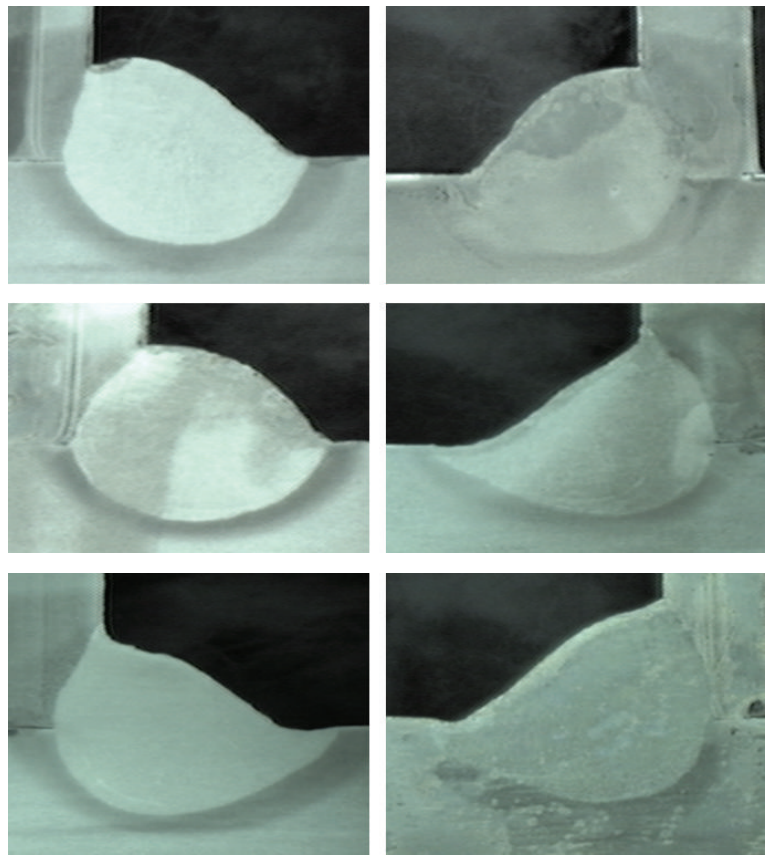

Figure 4: Some examples of macrophotographs of weld bead.

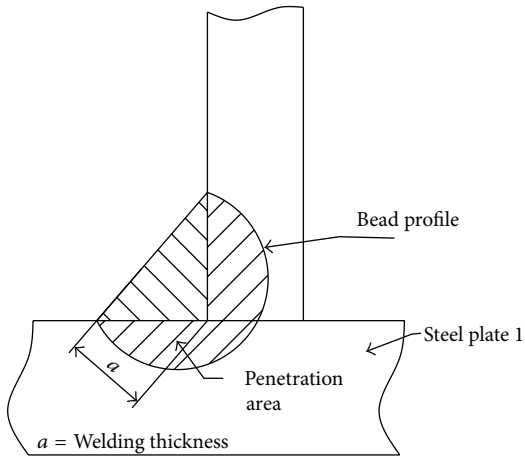

Figure 5: Cross-section of an ideal weld bead.

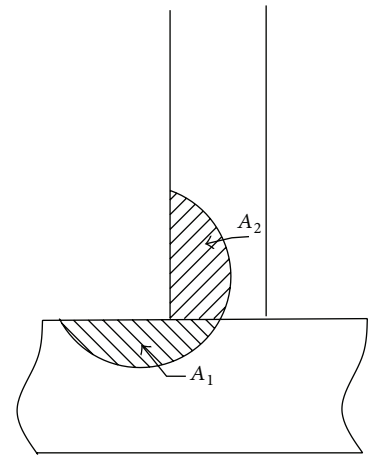

A_1 = The penetration area on the steel plate 1
A_2 = The penetration area on the steel plate 2

Figure 6: The penetration areas of the parts.

3. Modelling and Numerical Analyses

The weld quality depends on the weld bead geometry too much. To know correct machine setting that ensures satisfactory weld quality for a welding process is difficult. Because there is no known linear relationships between the desired bead geometry and the welding parameters. In other words, a good welding quality can be obtained if the bead geometry can be controlled by the process parameters. This case requires establishing a mathematical model of the relationship between the bead geometry and the welding parameters. Today, artificial intelligence technologies give this possibility. In this study, artificial neural network (ANN) and neurofuzzy approach are used and they are compared.

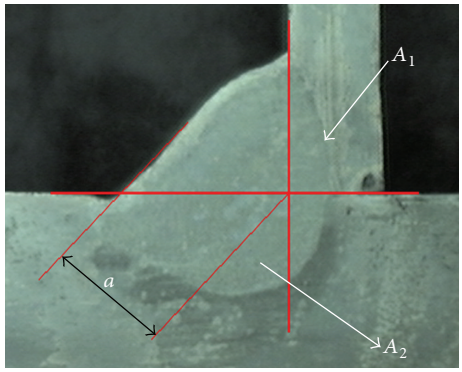

Figure 7: The bead geometry.

3.1. Artificial Neural Network (ANN). In this part of study, neural network model of submerged arc weld is established by using Neural Network Toolbox of MATLAB package. The input data consist of arc current, arc voltage, and welding speed. The output variables are welding thickness and penetration area. These output variables are individually considered and are modeled. Twenty-one data for training set and five data for testing set are used. The performance of training set for the welding thickness and the performance of testing set are shown in Figures 9 and 10, respectively.

For the penetration area, the performance of training set and the performance of testing set are shown in Figures 11 and 12, respectively.

3.2. Neurofuzzy Approach. Neurofuzzy systems combine the positive attributes of neural networks and fuzzy systems. Adaptive neuro fuzzy inference system (ANFIS) is used to the modeling of the SAW. There are three input parameters and two output values. In this study, the output values are considered individually, and so the models are prepared as three inputs and one output. The architecture of the ANFIS used in the proposed neurofuzzy approach is shown in Figure 13.

The same ANFIS model structure is used for the welding thickness and the penetration area. However, the different ANFIS editors are employed for the welding thickness and the penetration areas. The ANFIS editor used for the welding thickness is shown in Figure 14.

The ANFIS editor enables loading data, generating Fuzzy Inference System (FIS), training FIS, and testing FIS. Twenty-six experimental data of thirty-one welding process experiments listed in Table 2 are utilized to train the used ANFIS model, and five of them are utilized to test the model. The training and testing performance of the model are shown in Figure 14 and in Figure 15, respectively. The ANFIS model for the penetration area is developed by using similar procedure and the same input data have been used for this phase. Finally, the training performance and the checking performance for penetration area have been obtained in Figure 16 and in Figure 17, respectively.

4. Results and Discussion

Both ANN and ANFIS have given very suitable results. This case can be seen from the checking performance diagrams. From the comparison of the results obtained, it can be observed that the results of ANFIS are closer than the results of ANN to the experimental results. Therefore, to present the results of ANFIS is preferred and the effects of the welding thickness and penetration area are individually shown in Figures 18(a) and 18(b) and in Figures 19(a), 19(b), and 19(c), respectively. The input and the output values are reduced by using certain proportions. Therefore, the results of ANN and ANFIS must be extended with the same factors. This factor is 1000 for the arc current and the penetration area. For the arc voltage, the welding speed, and the welding thickness it is 100.

Experimental and theoretic results show that arc current, arc voltage, and welding speed affect penetration area and welding thickness in SAW process. Figure 18(a) shows the effect of interaction between arc voltage and arc current on welding thickness. It can be observed that the welding thickness increases with a decrease in arc voltage and an increase in arc current. But the maximum welding thickness is obtained when arc voltage is of minimum value and arc current is of maximum value. Also, the minimum arc current and the maximum arc voltage correspond to the minimum welding thickness. Figure 18(b) presents the effect of interaction between arc voltage and welding speed on welding thickness. It can be seen that the welding thickness increases with a decrease in arc voltage and in welding speed. The minimum welding thickness corresponds to the maximum values of arc voltage and arc current. However, the maximum welding thickness occurs when welding speed and arc voltage are minimum value.

Figures 19(a), 19(b), and 19(c) present the effects of the welding parameters on bead penetration area. Figure 19(a) shows that the penetration area is almost stationary up to 0,31 are voltage values, and it has a tendency to increase when arc current is 0,35 and arc voltage is higher than 0,31. The minimum penetration area occurs when voltage is maximum value and arc current is of minimum value. As seen from Figure 19(b), the penetration area increases with an increase in arc voltage and welding speed and it reaches the maximum value when welding speed and voltage are the maximum values. The minimum value of penetration area occurs when welding speed is of minimum value and arc voltage is 0,3. Figure 19(c) shows that the penetration area increases with an increase in arc voltage and welding speed, and it reaches the minimum value where arc current and welding speed are minimum values. On the contrary, the penetration area is the maximum value where arc current and welding speed are the maximum values.

5. Conclusions

In this study, it is aimed to obtain a relationship between the values defining bead geometry and the welding parameters and to select optimum welding parameters. For this reason, an experimental study has been realized. Also, modeling and analysis of the weld bead geometry in submerged arc welding by using adaptive neurofuzzy inference system have been performed. The major conclusions drawn from this study are the following.

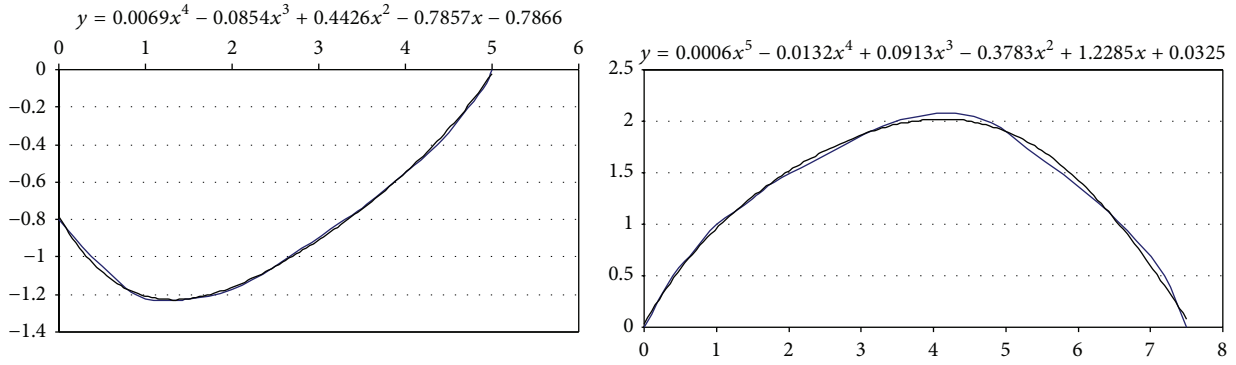

(a) Macro 1: Area 1 (A1).

(b) Macro 1: Area 2 (A2).

FIGURE 8: The polynomial equations representing the limit penetration profile of weld bead.

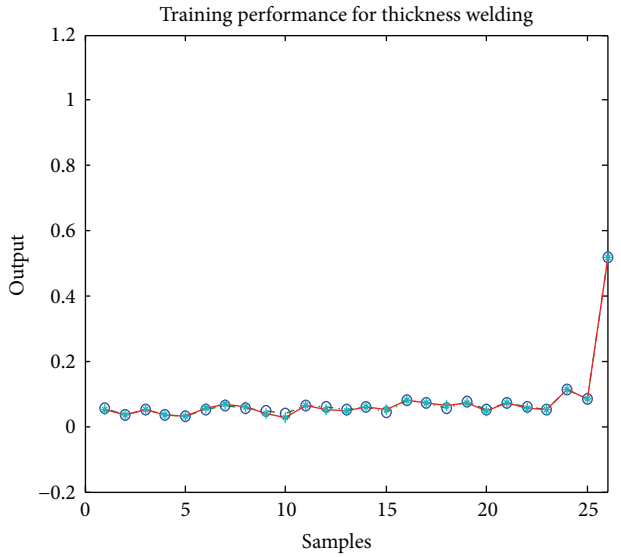

FIGURE 9: The performance of training set for the welding thickness.

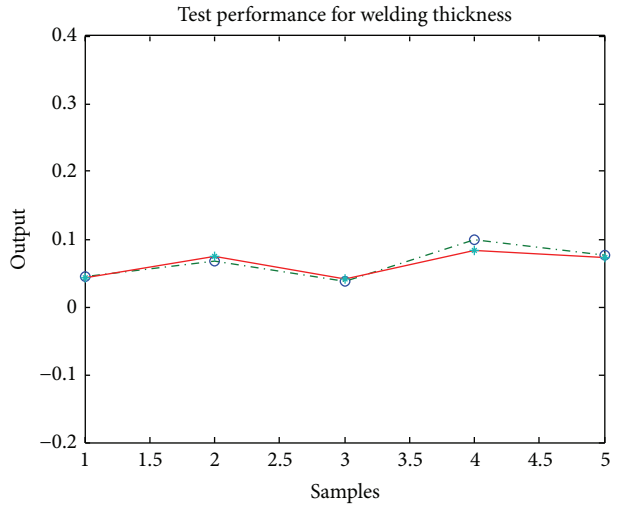

FIGURE 10: The performance of test set for the welding thickness.

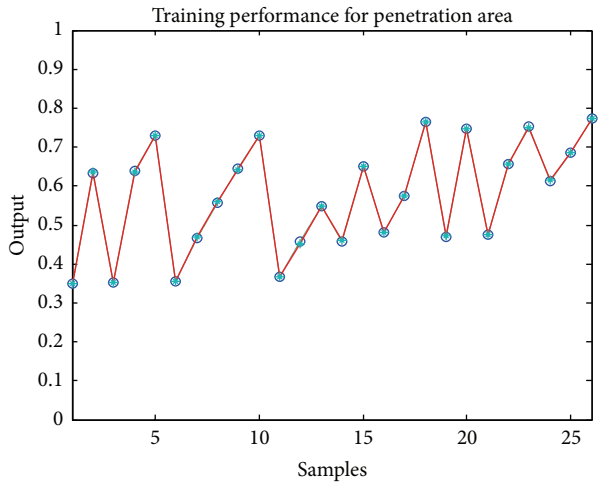

FIGURE 11: The performance of training set for the penetration area.

(i) ANN and ANFIS results are very close each other. But the results of ANFIS are closer than the results of ANN to the experimental results.

(ii) The experimental and theoretical results show that arc current, arc voltage, and welding speed affect penetration area and welding thickness in SAW process.

(iii) It can be observed that the welding thickness increases with a decrease in arc voltage and an increase in arc current. But the maximum welding thickness is obtained when arc voltage is of minimum value and arc current is of maximum value.

(iv) The minimum arc current and the maximum arc voltage correspond to the minimum welding thickness.

(v) The welding thickness increases with a decrease in arc voltage and in welding speed.

(vi) The minimum welding thickness corresponds to the maximum values of arc voltage and arc current.

(vii) The maximum welding thickness occurs when welding speed and arc voltage are of minimum value.

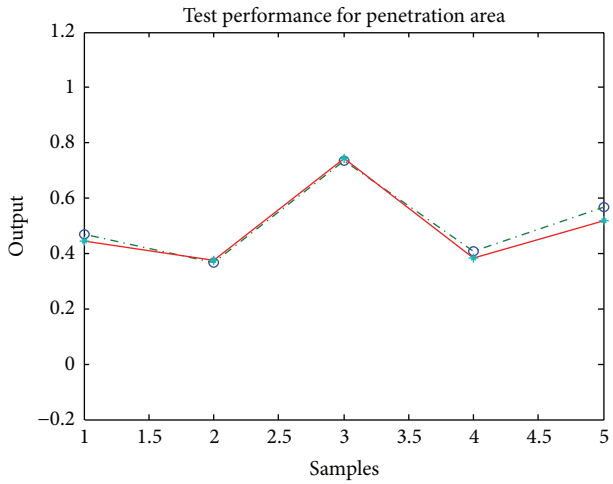

FIGURE 12: The performance of testing set for the penetration area.

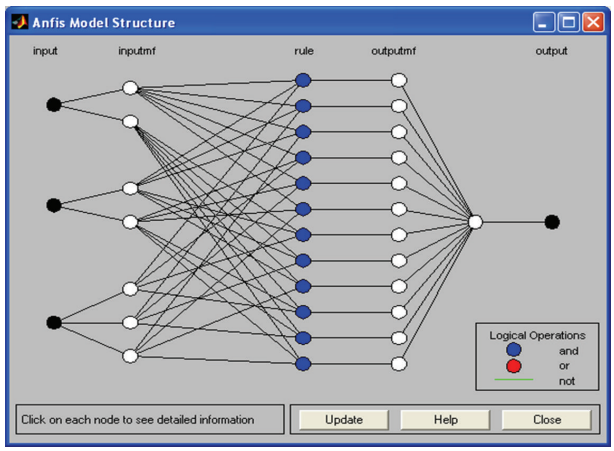

FIGURE 13: The architecture of the ANFIS used in the proposed approach.

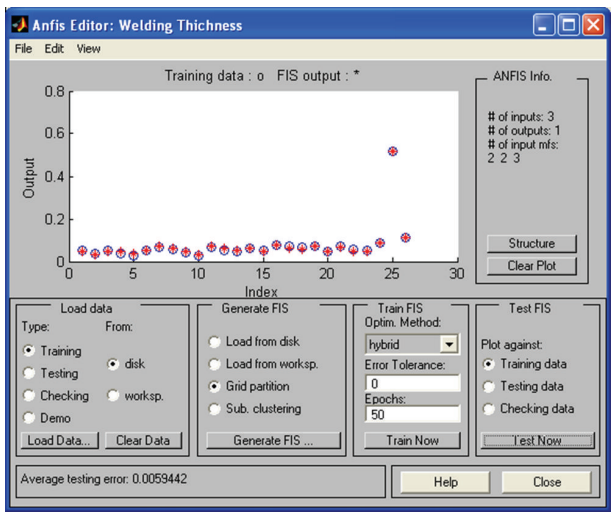

FIGURE 14: The training performance for the welding thickness.

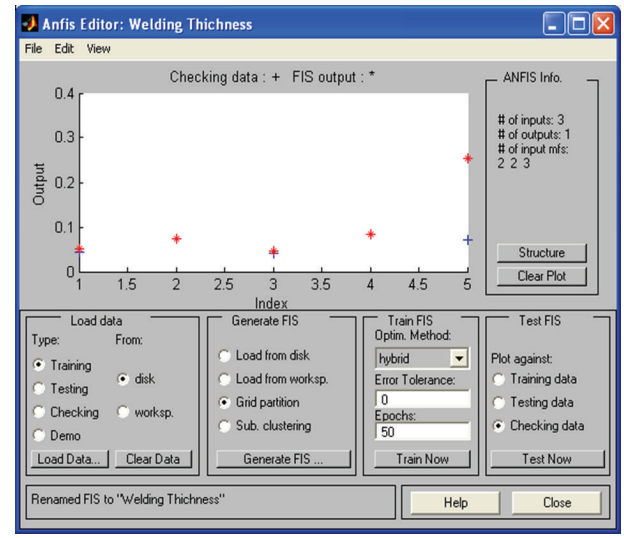

FIGURE 15: The checking performance for the welding thickness.

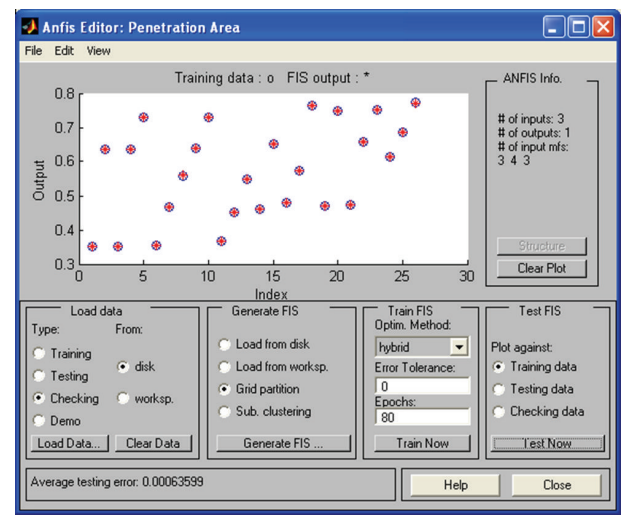

FIGURE 16: The training performance for penetration area.

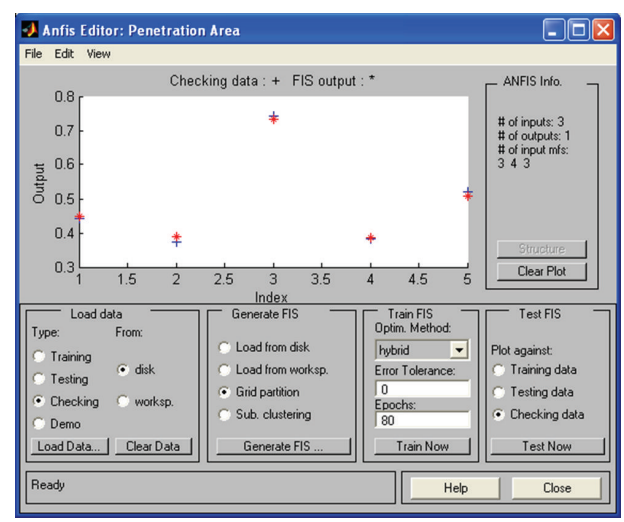

FIGURE 17: The checking performance for penetration area.

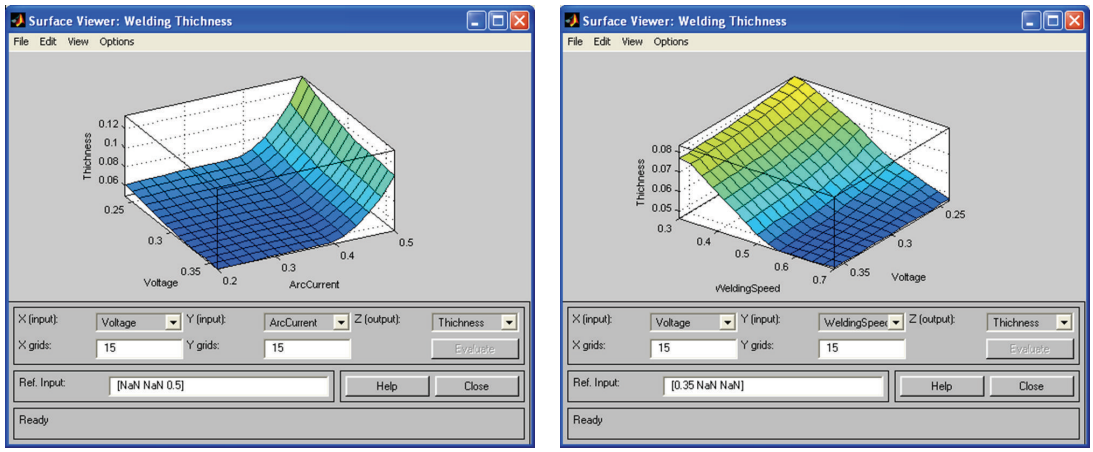

(a) (b)

Figure 18: (a) The effect of arc voltage and arc current on welding thickness. (b) The effect of welding speed and arc voltage on welding thickness.

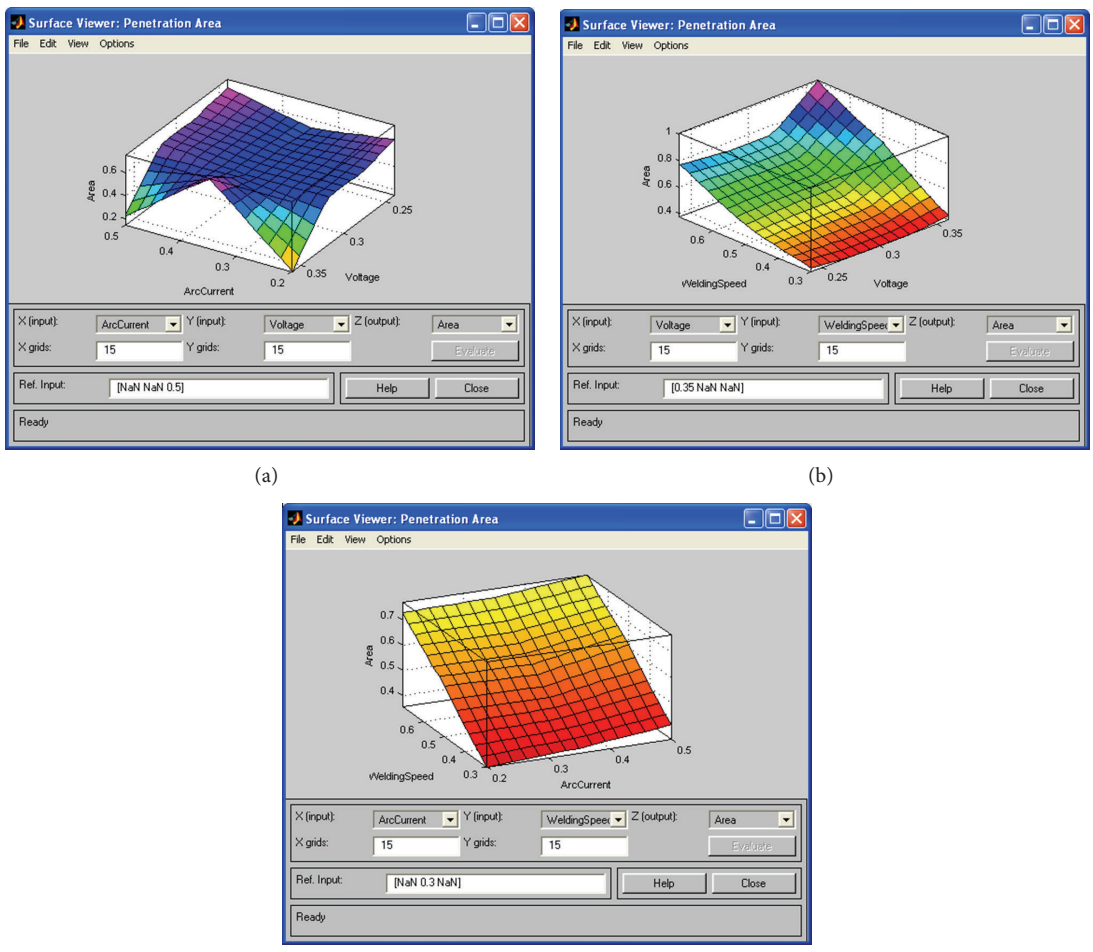

(a) (b)

(c)

Figure 19: (a) The effect of arc voltage and arc current on penetration area. (b) The effect of arc voltage and welding speed on penetration area. (c) The effect of arc current and welding speed on penetration area.

(viii) The penetration area is almost stationary up to 0,31 are voltage values, and it has a tendency to increase when arc current is 0,35 and arc voltage is higher than 0,31.

(ix) The minimum penetration area occurs when voltage is of maximum value and arc current is of minimum value.

(x) The penetration area increases with an increase in arc voltage and welding speed, and it reaches the maximum value when welding speed and voltage are the maximum values.

(xi) The minimum value of penetration area occurs when welding speed is of minimum value and arc voltage is 0,3.

(xii) The penetration area increases with an increase in arc voltage and welding speed, and it reaches the minimum value where arc current and welding speed are minimum values. On the contrary, the penetration area is the maximum value where arc current and welding speed are the maximum value.

It has been shown that submerged arc welding (SAW) process can be modeled by using artificial intelligence technologies. Finally, the models developed are able to predict the welding parameters required to obtain the desired bead geometry. This study can help to develop an intelligence control system for SAW process.

References

[1] R. S. Chandel, H. P. Seow, and F. L. Cheong, "Effect of increasing deposition rate on the bead geometry of submerged arc welds," *Journal of Materials Processing Technology*, vol. 72, no. 1, pp. 124–128, 1997.

[2] P. Li, M. T. C. Fang, and J. Lucas, "Modelling of submerged arc weld beads using self-adaptive offset neutral networks," *Journal of Materials Processing Technology*, vol. 71, no. 2, pp. 288–298, 1997.

[3] V. Gunaraj and N. Murugan, "Application of response surface methodology for predicting weld bead quality in submerged arc welding of pipes," *Journal of Materials Processing Technology*, vol. 88, no. 1, pp. 266–275, 1999.

[4] V. Gunaraj and N. Murugan, "Prediction and comparison of the area of the heat-affected zone for the bead-on-plate and bead-on-joint in submerged arc welding of pipes," *Journal of Materials Processing Technology*, vol. 95, no. 1–3, pp. 246–261, 1999.

[5] J. Tušek, "Mathematical modeling of melting rate in twin-wire welding," *Journal of Materials Processing Technology*, vol. 100, no. 1, pp. 250–256, 2000.

[6] H. C. Wikle III, S. Kottilingam, R. H. Zee, and B. A. Chin, "Infrared sensing techniques for penetration depth control of the submerged arc welding process," *Journal of Materials Processing Technology*, vol. 113, no. 1–3, pp. 228–233, 2001.

[7] N. Murugan and V. Gunaraj, "Prediction and control of weld bead geometry and shape relationships in submerged arc welding of pipes," *Journal of Materials Processing Technology*, vol. 168, no. 3, pp. 478–487, 2005.

[8] Y. S. Tarng, S. C. Juang, and C. H. Chang, "The use of grey-based Taguchi methods to determine submerged arc welding process parameters in hardfacing," *Journal of Materials Processing Technology*, vol. 128, no. 1–3, pp. 1–6, 2002.

[9] P. Kanjilal, T. K. Pal, and S. K. Majumdar, "Combined effect of flux and welding parameters on chemical composition and mechanical properties of submerged arc weld metal," *Journal of Materials Processing Technology*, vol. 171, no. 2, pp. 223–231, 2006.

[10] E. Nart and Y. Celik, "A practical approach for simulating submerged arc welding process using FE method," *Journal of Constructional Steel Research*, vol. 84, pp. 62–71, 2013.

[11] D. Zhao, Y. Wanga, Z. Lin, and S. Sheng, "An effective quality assessment method for small scale resistance spot welding based on process parameters," *NDT & E International*, vol. 55, pp. 36–41, 2013.

[12] D. W. Cho, W. H. Song, M. H. Cho, and S. J. Na, "Analysis of submerged arc welding process by three-dimensional computational fluid dynamics simulations," *Journal of Materials Processing Technology*, vol. 213, pp. 2278–2291, 2013.

[13] B. Acherjee, S. Mondal, B. Tudu, and D. Misra, "Application of artificial neural network for predicting weld quality in laser transmission welding of thermoplastics," *Applied Soft Computing Journal*, vol. 11, no. 2, pp. 2548–2555, 2011.

[14] S. Shen, I. N. A. Oguocha, and S. Yannacopoulos, "Effect of heat input on weld bead geometry of submerged arc welded ASTM A709 Grade 50 steel joints," *Journal of Materials Processing Technology*, vol. 212, no. 1, pp. 286–294, 2012.

[15] M. Leitner, T. Fössl, M. Stoschka, and W. Eichlseder, "Evaluation of fillet weld properties and fatigue behaviour in dependence of welding parameters," *Archives of Civil and Mechanical Engineering*, vol. 11, no. 3, pp. 651–660, 2011.

[16] D. S. Nagesh and G. L. Datta, "Genetic algorithm for optimization of welding variables for height to width ratio and application of ANN for prediction of bead geometry for TIG welding process," *Applied Soft Computing Journal*, vol. 10, no. 3, pp. 897–907, 2010.

[17] P. Sathiya, K. Panneerselvam, and R. Soundararajan, "Optimal design for laser beam butt welding process parameter using artificial neural networks and genetic algorithm for super austenitic stainless steel," *Optics and Laser Technology*, vol. 44, no. 6, pp. 1905–1914, 2012.

[18] J. E. R. Dhas and S. Kumanan, "Optimization of parameters of submerged arc weld using non conventional techniques," *Applied Soft Computing Journal*, vol. 11, no. 8, pp. 5198–5204, 2011.

[19] R. Sudhakaran, V. VeL Murugan, K. M. Senthil Kumar et al., "Effect of welding process parameters on weld bead geometry and optimization of process parameters to maximize depth to width ratio for stainless steel gas tungsten arc welded plates using genetic algorithm," *European Journal of Scientific Research*, vol. 62, no. 1, pp. 76–94, 2011.

[20] J. E. R. Dhas and S. Kumanan, "Optimization of parameters of submerged arc weld using non conventional techniques," *Applied Soft Computing Journal*, vol. 11, no. 8, pp. 5198–5204, 2011.

[21] P. Sreeraj and T. Kannan, "Modelling and prediction of Stainless steel clad bead geometry deposited by GMAW using regression and artificial neural network models," *Advances in Mechanical Engineering*, vol. 2012, Article ID 237379, 12 pages, 2012.